

THIS REPORT HAS BEEN DELIMITED
AND CLEARED FOR PUBLIC RELEASE
UNDER DOD DIRECTIVE 5200.20 AND
NO RESTRICTIONS ARE IMPOSED UPON
ITS USE AND DISCLOSURE.

DISTRIBUTION STATEMENT A

APPROVED FOR PUBLIC RELEASE;
DISTRIBUTION UNLIMITED.

UNCLASSIFIED

AD 403 091

*Reproduced
by the*

DEFENSE DOCUMENTATION CENTER

FOR

SCIENTIFIC AND TECHNICAL INFORMATION

CAMERON STATION, ALEXANDRIA, VIRGINIA



Best Available Copy

UNCLASSIFIED

NOTICE: When government or other drawings, specifications or other data are used for any purpose other than in connection with a definitely related government procurement operation, the U. S. Government thereby incurs no responsibility, nor any obligation whatsoever; and the fact that the Government may have formulated, furnished, or in any way supplied the said drawings, specifications, or other data is not to be regarded by implication or otherwise as in any manner licensing the holder or any other person or corporation, or conveying any rights or permission to manufacture, use or sell any patented invention that may in any way be related thereto.

403091

Reprinted from APPLIED OPTICS, Vol. 2, page 190, February 1963.
Copyright 1963 by the Optical Society of America, and reprinted by permission of the copyright owner.

Reduction of Scattered Light in the Coronagraph

Gordon Newkirk, Jr., and David Bohlin

HIGH TECH. CENTER
NORBERT
LABORATORY
393 (10)

AS AL NO
UNIVERSITY OF COLORADO

Introduction

Until the development of the coronagraph by Lyot¹ three decades ago, the solar corona was visible for only a few minutes every year during total eclipse. It was demonstrated during the International Geophysical Year,² the several Lyot coronagraphs placed on mountaintops around the world were able to provide a reasonably continuous record of the emission line corona within the first 100,000 km (3.3 solar radii) of the solar limb. However, the relation of the outer corona (Fig. 1) to the more easily observable inner part is still unclear. If the corona and its connection with the interplanetary medium are to be understood, the region of frequent observation must be extended to several solar radii. At present, occasional images of the corona to one solar radius above the limb have been built up by scanning with the K-coronameter.³ Except for the analysis of occasional occultations of radio stars, the study of radio noise of coronal origin, and the infrequent penetration of space probes, the structure of the outer corona is still unknown outside of eclipse.

More frequent, high-resolution pictures of the corona should be made during a period of several weeks or months. It would then be possible to study not

Gordon Newkirk, Jr. is at the High Altitude Observatory, National Center for Atmospheric Research and is Professor Adjunct at the University of Colorado. David Bohlin is in the Department of Astrophysics, University of Colorado, Boulder, Colorado.

Received 21 September 1962

This research was supported in part by the auspices of an Office of Naval Research grant.

The development of balloon and rocket vehicles provides opportunity for nearly continuous observation of those parts of the solar corona remote from the sun. This opportunity places new requirements on the freedom of the coronagraph from scattered light. Several possible means of improving the coronagraph are described. It is found that the available optical media do not permit a significant reduction in the scattered light in the ordinary coronagraph. The reflecting coronagraph and the simple, externally occulted coronagraph can be made free of scattered light by from one to more than two orders of magnitude, respectively, than the Lyot coronagraph. The use of the apolized, external, occulting disk developed by several investigators can reduce the scattered light by at least three orders of magnitude so that the instrumental background is similar to the skylight encountered during total eclipse.

only such short-lived, transient changes in the corona as may follow solar flares, but also the more gradual changes which accompany the formation and decay of the solar active regions. By placing an improved version of the coronagraph above the atmosphere in either a balloon or an orbiting solar observatory, we can hope to realize the long sought for opportunity of nearly continuous observation. Moreover, improved coronagraphs will assist in the solution of planetary atmosphere problems, in the search for planets accompanying nearby stars, or in any other experiment in which a faint source must be distinguished from a close, bright one.

It is valuable to examine the freedom from scattered light that is required of any coronagraph used above the atmosphere. The Lyot coronagraph, although it allows a reduction of the scattered light by at least a factor of 100 below that contributed by the best of simple telescopes, still scatters light of radiance approximately 5×10^{-6} that of the mean solar disk. Since the radiance of the sky seen from high mountaintops on the clearest days^{4,5} is approximately 10^{-5} in the green, the Lyot coronagraph is completely adequate for use at any ground-based observatory. At such stations only the inner corona with a radiance of the order of 10^{-6} is accessible to direct observation. Since the corona can be photographed directly only when it has a radiance at least 10% in excess of the background, examination of the corona to six solar radii requires reduction of the background to approximately 10^{-7} . This lower level of scattering is a realistic goal for the improvement of the coronagraph.

The performance of the satellite-borne coronagraph

403091

APPLIED OPTICS, Vol. 2, No. 2, February 1963

February 1963 / Vol. 2, No. 2 / APPLIED OPTICS 191

Best Available Copy



S

Fig. 1. The solar corona as depicted in an original drawing by the late Mr. Wesley, Secretary of the Royal Astronomical Society. The drawing was made from the negative of a photograph made by Mrs. Annie S. Maunder, who photographed the 22 January 1898 eclipse at Talni, Hyderabad on a Sandal triple-coated plate. The connection between the outer coronal streamers, which extended to an unusual distance in 1898, and active regions on the surface of the sun as well as magnetic storms on the earth remains a challenging mystery of solar physics.

is limited only by scattering within the instrument. The balloon-borne instrument can, in practice, be placed above only about 99% of the atmosphere, and it is necessary to examine the character of the skylight at high altitudes more closely. Measurement at altitudes of up to 25,000 m at wavelengths from 0.4 μ to 0.8 μ show a sky radiance of the order of 10^{-8} that of the mean solar disk.¹³ Comparison of the corona and the sky at 25,000 m, as in Fig. 2, suggests that at $\lambda = 1.2 \mu$ the corona should be visible to approximately four solar radii. To detect the corona at the desired six solar radii the sky background must be reduced by a factor of three by carrying out the observations at an altitude of 33,000 m.

Before describing the techniques by which the scattered light in the coronagraph can be reduced to a radiance of the order of 10^{-9} that of the disk of the sun, a value that is only slightly above the sky encountered during a solar eclipse,¹⁴ we shall review the scattering produced in the traditional Lyot coronagraph.

Sources of Scattering in the Lyot Coronagraph

In his patient analysis of the scattering by a simple objective lens Lyot distinguished five sources of stray

light which can all be seen clearly in a lens illuminated by a synthetic sun (Fig. 3). As in the coronagraph the "solar image" is occulted by a disk, and the lens is viewed in the stray light which passes the disk. The sources of scattered light are:

1. Diffraction at the aperture of the objective lens. If unobstructed, this diffraction ring produces a radiance in the field of the coronagraph of approximately 2×10^{-4} of the mean solar radiance B_{\odot} .

2. A spurious solar image produced by multiple reflections in the objective lens. This image is about $1/6$ of the focal length away from the objective and introduces stray light of radiance

$$B \approx 6 \times 10^{-9} (f/D)^2 B_{\odot},$$

where f is the focal length of the objective and D its diameter. In Fig. 3 the central bright spot is slightly out of focus.

3. Macroscopic inhomogeneities in the glass. Small bubbles and inclusions produce many of the randomly distributed starlike spots in Fig. 3.

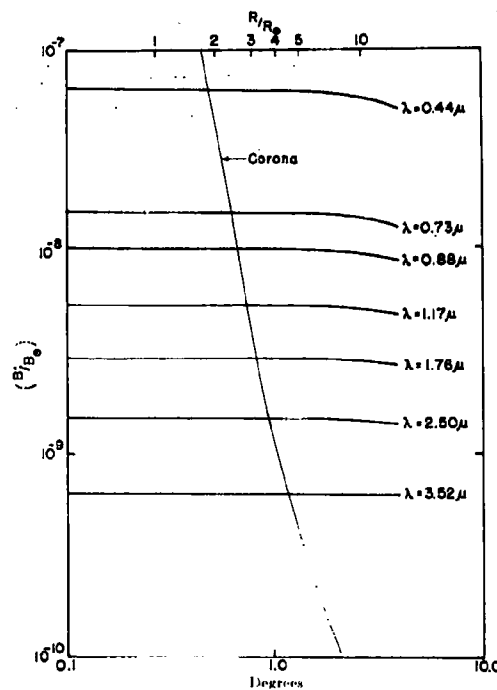


Fig. 2. A comparison of the radiance of the sky at 25,000 meters and of the solar continuum corona at several wavelengths. The radiances from 0.44 μ to 0.8 μ were measured¹³ while the values at longer wavelengths were inferred from the size distribution of the particles determined by means of the angular distribution of scattered light at visible wavelengths. Coronal radiances are plotted as a function of the distance from the center of the solar disk in units of the solar radius R_{\odot} .

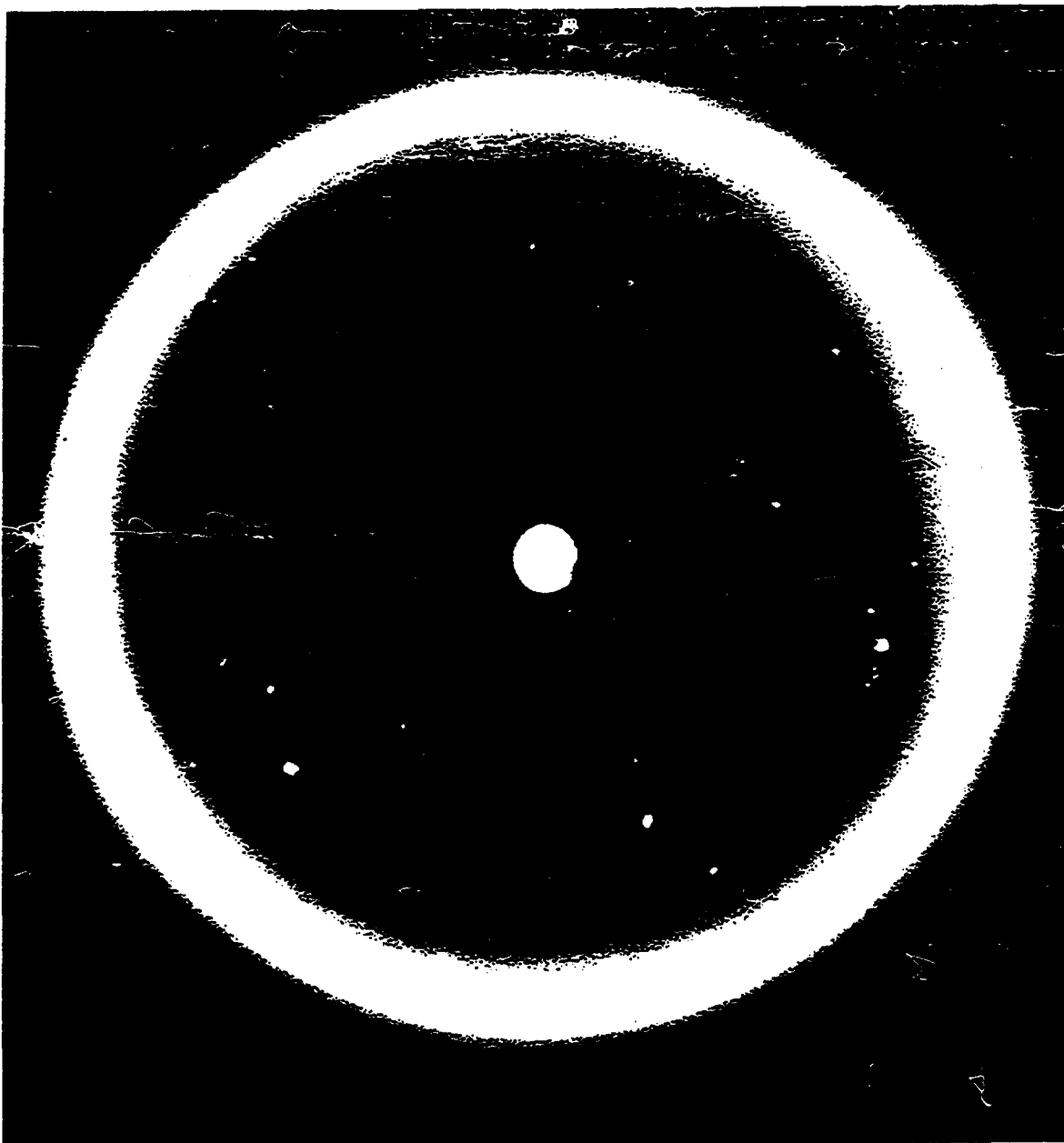


Fig. 3. Photograph of a coronagraph lens illuminated by a laboratory source of 32 mm of arc diameter. This particular lens produced stray light of radiance 3.3×10^{-2} that of the mean solar disk.

1. Departures of the surface of the lens from a uniform shape. Pits in the surface of the glass produce starlike images very similar to the bubbles within the glass. Also as departures of the surface from ideal shape we must include scratches on the glass and any other lack of perfection in polish or figure as well as dust residing temporarily on the surface.

2. Body scattering within the glass itself. This

source produces an apparently uniform haze over the entire aperture. We here distinguish between the macroscopic inhomogeneities in the glass, such as large bubbles and striations (source 3a), and microscopic inhomogeneities.

Lyot found that by using a field lens to image the objective on an aperture which did not pass the bright diffraction ring and by eliminating the multiple re-

Table I. Comparison of Scattering by Sample Coronagraph Lenses

Glass type	Sample no.	Manufacturer	Striae	Granulation	Surface	Bubbles	Fluorescence	B/B_0 (10^{-6}) for $\lambda = 0.51 \mu$
<i>Samples free of obvious surface defects and striations</i>								
BSC-2	3	Corning	Absent	Weak	Good	Very few	Faint yellow	1.2
Fused silica (Schlieren grade)	3	Corning	Absent	Weak	Good	Very few		1.7
BK-7	2	Schott	Absent	Medium	Good	Few		2.4
BK-7	1	Schott	Absent	Medium	Good	Few		2.5
Ultrasil	2	Engelhard	Absent	Medium- strong	Good	Few		2.5
PK-2	1	Schott	Absent	Medium	Good	Few		3.3
Fused silica (Schlieren grade)	1	Corning	Absent	Weak	Pits?	Several		4.2
Ca F ₂	1	Harshaw	Absent	Severe	Sleeks?	Medium	Strong blue	21
<i>Samples with defects</i>								
BSC-2	1	Corning	Wide- band	Medium	Good	Few	Faint yellow	2.8
Ultrasil	1	Engelhard	Absent	Medium- strong	Scratch	Few		3.1
BSC-2	2	Corning	Band	Medium	Good	Few	Faint yellow	3.1
BK-7	3	Schott	Absent	?	Poor polish	Few		5.6
L-4	1	Schott	Absent	Medium	Faint scratch	Several	Faint blue	5.7
Ba-SFS-1	1	Schott	Absent	?	Etched by cleaning in water	?	Strong yellow	33

flexion spot by placing a small occulter on the center of the second objective lens he was able to reduce the stray light in the coronagraph to about 5×10^{-6} . He concluded that most of the residual illumination is due to the scattering by the inevitable bubbles and inclusions and by the body-scatter of the glass. Since the technology of glassmaking has advanced considerably in the intervening 30 years, it appears fruitful to seek an optical medium that can be fashioned into a coronagraph lens with considerably less scattering.

Scattering in Various Optical Media

It must be remembered that forward scattering by the imperfections of the objective lens is of great importance in the coronagraph. Thus, scattering by large bubbles and by irregularities of microscopic (0.5μ to 100μ) dimensions completely dominates that from any irregularities of atomic (1 \AA to 10 \AA) scale. This fact is emphasized by the observation that objective-lens scattering is many orders of magnitude higher than one would expect from the random density fluctuations inherent in the glass.¹⁵

With this information in mind we can place some very general requirements on the medium for a coronagraph lens in approximately the following order of importance:

1. Absence of striations, bubbles, and inclusions.
2. Ability to take a fine polish and to resist scratches during cleaning (hardness).
3. Absence of fluorescence in the spectral region of interest.
4. Resistance to etching by water, the common solvents, and various air-borne pollutants likely to be encountered during use.
5. Absence of birefringence.

These requirements suggest the use of several of the colorless, cubic crystals such as cristobalite, spinel, and diamond, which are hard enough to resist scratching. Unfortunately, large optical quality samples of these minerals are rare. Such minerals as fluorite (CaF₂), barium fluoride, and lithium fluoride, which can be obtained as large synthetic crystals of optical quality, are so soft that they are, in our experience, nearly impossible to polish to coronagraph quality.

We have tested several samples of modern glasses by using each one as the objective (2.5 cm diameter; 25 cm focal length) of a small, laboratory coronagraph. Radiation from the entire coronagraph field of diameter of approximately eight solar radii was recorded by a photomultiplier, which was calibrated by a series of opal glasses of known surface radiance placed before the objective. Comparison between independent measure-

ments indicates that the scattering from a particular sample is accurate to about 10%.

The results of these measurements appear in Table I in which the various lens samples are listed in order of their excellence. Since the varieties of glass were chosen for absence of bubbles, it is not surprising that only a few of the samples show a large amount of scattering. However, all the samples had some body-scattering in the form of a "granular structure." The fact that those lenses with the weakest granulation also scattered the least amount of light indicates that this structure contributes significantly to the scattering by the lens. Under high magnification the granular structure in the glasses and the fused silica can be recognized as a regime of minute bubbles which seem to be merely the lower size range of the spectrum of bubble sizes. The less frequent but larger bubbles can, of course, be recognized as individuals. Granulation in the fluorite sample, however, was of an entirely different character and appeared as a cellular structure distributed throughout the volume of the crystal.

Examination of Table I also shows that faint scratches and striae can add approximately 1.2×10^{-6} per scratch to the scattering. *One concludes that carefully selected blanks of the common crown glasses BSC-2 or BK-7 as well as the best grades of fused quartz make the best coronagraph objectives so far as scattering is concerned.* Although the LF-1 lens scatters significantly more than the best samples, it does not seem to deserve the bad reputation for high scattering usually associated with flint glass and could doubtless be used as a component in an achromatic coronagraph lens suitable for ground-based observation.

Although these optical media are transparent in the visible region, several of them absorb rather strongly at short wavelengths. Unfortunately, energy absorbed at short wavelengths may reappear in the form of fluorescence and contribute a significant amount to the stray light in the coronagraph field. This is illustrated by the case of diamond—apparently an otherwise suitable medium for coronagraph lenses which when irradiated by light of wavelength shorter than 2600 Å fluoresces in the blue or in the green.¹⁶ Several of the lens samples tested for scattering also exhibit fluorescence in the visible (Table I). The glasses containing somewhat loosely bound ions of boron, barium, and lead, within the SiO₂ network of the glass have strong absorption in the 2000 to 3000 Å region and show the strongest fluorescence.¹⁷ Although we have made no comparison on an absolute intensity basis, the fluorescence of BSC-2 glass suggests that this otherwise excellent lens medium should not be used in a coronagraph operated completely above the atmosphere where the ambient, ultraviolet flux is extremely high. In fact, even fused quartz fluoresces under exposure to sufficiently short wavelength radiation. The design of

a satellite-borne coronagraph should be made with the possible hazard of fluorescence in mind. A coronagraph at balloon altitudes is protected from radiation short of 3000 Å by the overlying ozone absorption, and the selection of a lens free from fluorescence is correspondingly easier.

Reflecting Coronagraphs

One concludes from the preceding section that minute bubbles within even the best glasses prevent the construction of coronagraph lenses of close to theoretical performance so far as light scattering is concerned. In the reflection coronagraph the pinholes, minute hills, and granular structure that appear in metals deposited on glass scatter more radiation than the imperfections within the glass of the ordinary system.¹⁸ Until new techniques of depositing completely uniform coatings of metal on glass or of producing polishable metals of high quality are developed to a sufficient standard of excellence, the uncoated mirror offers a useful alternative. The mirror coronagraph with uncoated primary surface takes advantage of the excellent polish which can be given to such media as glass or quartz as well as the fortunate circumstance that the bubbles in the medium scatter principally in the forward direction. Our tests of the scattering from a sample of fused quartz show that the advantage of low backscatter more than compensates for the disadvantage of the small reflectivity of the primary surface. The scattered light in such a coronagraph should be at least an order of magnitude smaller than in the objective lens coronagraph. We are presently investigating the practicality of such a reflecting system.

Disposal of the unwanted radiation passing through the primary surface can, of course, be a problem. The use of an opaque glass or an antihalation coating on the back surface is likely to heat the mirror excessively and cause distortion of its figure. However, very simple schemes, such as shown in Fig. 1, allow most of the radiation to pass through the mirror to a light trap while only 4% of the incoming flux must be absorbed

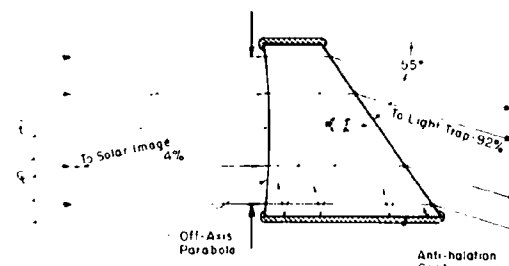


Fig. 1. The mirror for a reflection coronagraph in which stray reflections are greatly reduced.

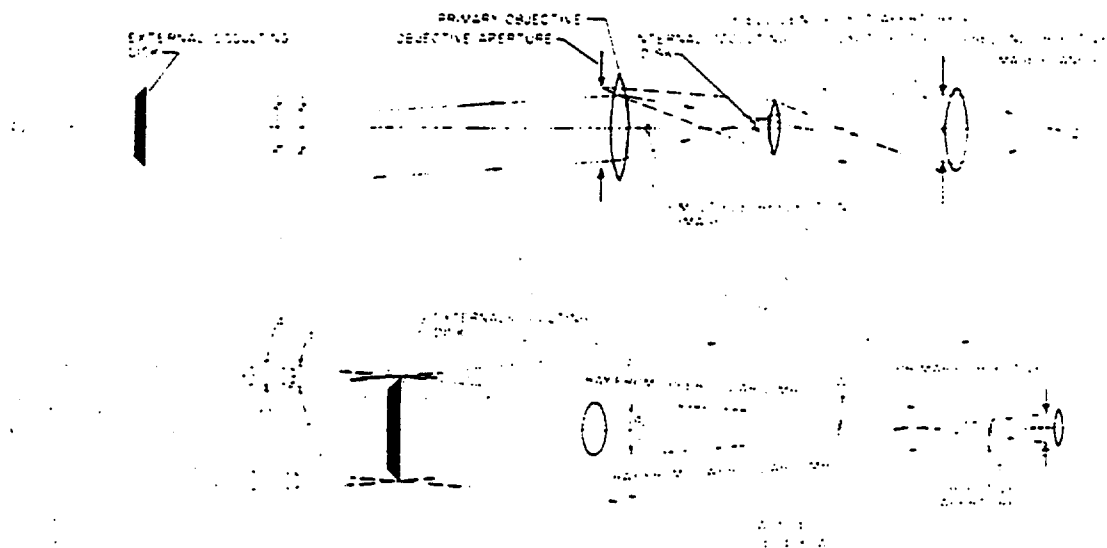


Fig. 5. (a) Schematic diagram of the externally occulted coronagraph. The occulting disk prevents direct photospheric light from falling on the primary objective lens while a second disk blocks the bright diffraction image of the first occulting disk. Light diffracted at the objective aperture is brought to a focus on the Lyot aperture by the field lens. A small spot in the center of the second objective blocks the multiple reflection image of the external occulting disk. (b) Geometry of the external occulting. The angular diameter δ of the occulting disk must exceed that of the sun by Δ .

in the antireflection coating. The high efficiency of antireflection layers with the same refractive index, as that of the mirror (e.g., Laxorb[®]) allows the stray light within the mirror to be reduced to from 1×10^{-2} to 1×10^{-4} of the incoming intensity after one reflection from a treated face. Reflection off a second treated face reduces this quantity by another factor of from 10^{-2} to 10^{-4} .

Externally Occulted Coronagraphs

Although the previous two sections suggest that the scattered light in the coronagraph can be substantially reduced, we must conclude that, at the present time, the necessary several orders of magnitude improvement over the Lyot coronagraph required of the satellite or balloon-borne systems can only be accomplished by shielding the objective lens from direct photospheric radiation. The most practical means of doing this is with an external occulting disk.

The first to suggest a coronagraph with an external occulting disk was John W. Evans. A sky photometer based on Evans' design was used by one of us to study the solar annode from various mountain peaks. A modification of this externally occulted coronagraph has been flown to altitudes of 25,000 m³ to determine the variation of sky radiance with angle from the sun, wavelength, and altitude.

The nature of the externally occulted coronagraph (Fig. 5a) requires that d , the angular diameter of the

occulting disk as seen from the objective, exceed that of the sun, δ , by an amount, Δ , which is just the angular diameter of the objective lens as seen from the occulting disk. The reason for this requirement is clear from Fig. 5b. The fact that the corona within the diameter d_1 is vignettted may be used in some cases partially to compensate the sharp decrease of coronal radiance with increasing distance above the solar limb. The advantage of having the occulting disk supported far in front of the objective lens is that the corona can be examined close to the solar limb. However, the impracticality of using an external occulting disk on a ground-based coronagraph of, say 15 cm aperture, can be seen from the fact that the disk must be 292 m away from the objective if the corona is to be examined as close as two minutes of arc of the limb.

Measurement shows that the stray light in an externally occulted coronagraph is about 10^{-4} of the mean solar disk. Although this represents an improvement factor of approximately 500 over the Lyot coronagraph, it is still an order of magnitude too large for meaningful coronal photography above the atmosphere. The major source of this residual stray light is diffraction by the occulting disk.

One obvious method of decreasing the scattered light in the externally occulted coronagraph is to increase the size of the occulting disk without correspondingly increasing the diameter of the objective lens. That such occulting does reduce the flux onto the objective

lens is shown in Fig. 6. Such a device is rather impractical since the occulting disk also blocks most of the corona. A more subtle artifice is to apodize the occulting disk.

The technique of apodization^{22, 23} can be used to modify the diffraction pattern about the Gaussian image point of a lens by a suitable variation of the transmission across the lens. The same technique, under the name of "antenna tapering," has been used by radio engineers to suppress the side lobes of the patterns of radio interferometers. The aperture stop at the second objective of the Lyot coronagraph produces, in a very real sense, an apodization of the objective lens in which resolution is sacrificed for a dramatic decrease in the diffraction far from the Gaussian image point. An analogous problem is that of the apodization of the occulting disk except that the conditions of Fresnel rather than Fraunhofer diffraction apply. Here one desires to reduce the light diffracted by the external occulting disk into the aperture of the objective lens by a suitable "tapering" of the disk outside the limb of the sun.

A point source illuminating a disk produces a bright spot in the center of the shadow. This bright spot is seen in Fig. 7. If a means can be found to eliminate the central spot behind the occulting disk, the major source of stray light in the externally occulted coronagraph can be removed.

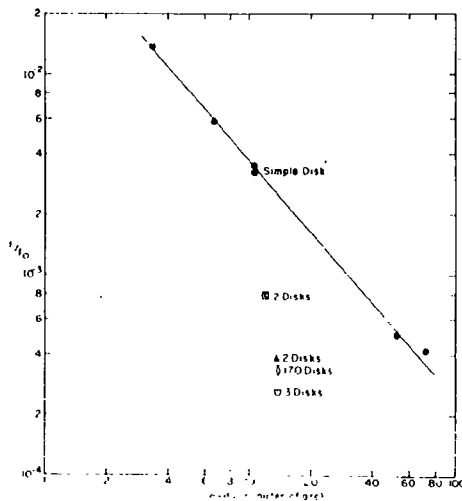


Fig. 6. Reduction of the flux into an objective aperture 1.2-mm diameter placed 76 cm behind various occulting disks. Here F is the flux observed with the occulting disk in place, while F_0 is the flux in the unobstructed beam. The reduction is plotted as a function of the difference between the diameter of the occulting disk and the diameter of the sun in min of arc. The synthetic sun was a ribbon filament lamp whose objective lens subtended an angle of 32 min of arc from the objective aperture.



Fig. 7. The distribution of light in the shadow of a circular occulting disk illuminated by a point source. The familiar, bright, central spot is predicted by the Fresnel diffraction theory. The radial lines are caused by minute irregularities in the edge of the occulting disk.

To see that the bright, central spot can be removed in principle, consider the amplitude at the point P illuminated by a point source P_0 . By the Fresnel theory the amplitude at P is²⁴

$$U(P) = 2\sqrt{\lambda} \frac{A_0 e^{ikr_0 + i\pi/4}}{r_0 + b} \sum_{l=1}^n C_l U^{(l)}(\chi_l) \quad (1)$$

where

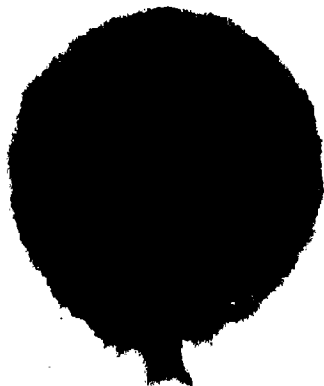
- A_0 = amplitude of the incident wave at unit distance from the source,
- r_0 = radius of the wave front from P_0 ,
- b = distance from P to the nearest point of the wave front,
- $k = 2\pi/\lambda$,
- χ_l = the inclination factor that describes the variation of amplitude of the secondary wavelets with angle of diffraction χ .

The usual development makes use of the fact that χ is a smoothly decreasing function of χ and tends to zero as $\chi \rightarrow \pi/2$, ($l \rightarrow n$). If a circular obstruction covers the first $j-1$ Fresnel zones, the summation in (1) is written

$$U = 1 + \sum_{l=j}^n C_l U^{(l)}(\chi_l) = \frac{\chi_j}{2} + \left(\frac{\chi_j}{2} - \chi_{j+1} \right) \frac{\chi_{j+1} + 2}{2} + \left(\frac{\chi_{j+1} + 2}{2} - \chi_{j+2} \right) \frac{\chi_{j+2} + 2}{2} + \dots \quad (2)$$



(a)



(b)

Fig. 8. The distribution of light in the shadow of a multiple-occluding disk (a) and a toothed wheel (b) illuminated by a point source. The disappearance of the bright central spot is obvious. The multiple-occluding disk was calculated so that the objective aperture would be completely contained in the central dark region of the shadow.

Following the argument, we note that the terms in parentheses are vanishingly small since

$$k_{j+1} \ll k_{j+2}$$

and

$$k_{j+1} \ll 1 \ll \sum_{k=1}^j (1 \pm k) \approx \frac{j^2}{2}, \quad (3)$$

a classical result.

Consider, now, that although the first $j-1$ zones are blocked, the zones from j to m are not completely clear but obscured by an apodization factor a_k . Corresponding to Eq. (2) we have

$$\begin{aligned} & (1 \pm 1)^{j+1} \sum_{k=1}^m (1 \pm 1)^{k-1} k! \approx \frac{k^m}{2} \\ & \cdot \left(\frac{k a_k}{2} - k_{j+1} a_{j+1} + \frac{k_{j+2} a_{j+2}}{2} \right) \cdot \dots \\ & \cdot \left(\frac{k m - 2}{2} a_m - 2 \frac{k m - 1}{2} a_{m-1} + \frac{k m - 2}{2} \right) \\ & \cdot \left(\frac{k m a_m}{2} - k_{m+1} + \frac{k m + 2}{2} \right) \\ & \cdot \left(\frac{k m + 2}{2} - k_{m+3} + \frac{k m + 1}{2} \right) \dots \quad (4) \end{aligned}$$

if $m-j$ is even. To retain the feature of the ordinary Fresnel diffraction theory we need only require that $a_j = a_{j+1}$ and $a_m = 1$. The usual argument concerning the vanishing of the bracketed terms still applies and

$$(1 \pm 1)^{j+1} \sum_{k=1}^m (1 \pm 1)^{k-1} k! \approx \frac{k^m}{2}.$$

A similar result holds for odd $m-j$.

Thus, the intensity at P is reduced by the factor a_j^2 , which, in principle, can be made arbitrarily small, and the central, bright spot (Fig. 7) can be substantially reduced in intensity. Although the illuminating source for a practical coronagraph has a finite solid angle, the problem is essentially the same with each point of the solar disk acting as a coherent source.

Several means of producing the apodization have been suggested. An ingenious scheme, due to Purcell and Koomen,²⁵ makes use of an occulting disk with sharp teeth which extend beyond its normal diameter. Although their explanation of the operation of such a disk—that the teeth diffract perpendicularly to their straight surfaces and thus do not scatter light into the objective aperture—does not emphasize the physics of the diffraction process, their requirement that the teeth have extremely sharp bottoms is seen to be a natural one from the mathematical development. A second form of the apodized occulting disk is one attached to a radially symmetric filter whose transmission changes from nearly zero at the edge of the completely opaque disk to unity at a larger radius. The obvious disadvantage of such a scheme—that irregularities in the

filter medium diffract light into the objective aperture would seem to prevent its use in a practical device. A third apodizing scheme makes use of a second occulting disk behind the first partially to obscure the objective lens as seen by the Fresnel zones immediately above the first occulting disk. Since the second occulting disk is illuminated by weak radiation diffracted by the first, it may in turn diffract radiation into the objective aperture. Thus, to make the obscuration factor a , sufficiently small, we may wish to add a third occulting disk behind the second. Since the toothed wheel as an external occulting disk has been thoroughly discussed by Purcell and Koomen,²⁵ we shall proceed immediately to the detailed description of the multiple disk.

As can be seen in Fig. 8, both the toothed wheel and the multiple occulting disk eliminate the bright diffraction spot in the center of the shadow. To make a quantitative comparison of these various occulting schemes we used a ribbon filament lamp as a synthetic sun and measured the light diffracted into a small aperture in the center of the shadow. The efficacy of the second occulting disk is immediately apparent in Fig. 9, which shows the reduction in the flux into the objective aperture as a function of the position of the second occulting disk. The maximum reduction occurs just when the second and smaller disk completely obscures the objective lens from the edge of the first disk. The addition of a third occulting disk produces a further reduction in the flux falling on the objective aperture. It is of interest to note that the use of only disks Nos. 1 and 3 of the three-disk configuration produces a somewhat poorer flux reduction than that accomplished by all three disks. The performance of these various occulting schemes is summarized in Table II. The logical extension of the three-disk occulter, an occulting disk with many components spaced between the positions of disks Nos. 1 and 3, performs somewhat less well than does the three-disk system. While the system with 170 disks should behave as well or better than the three-disk system, the inevitable irregularities in the disks undoubtedly throw spurious radiation into the objective aperture. Thus, by the use of a multiple occulting disk of appropriate design, we can bring about a reduction in the flux into the objective aperture of the

Table II. Comparison of Occulting Disks Illuminated by an Extended Source of 32 Min of Arc Diameter

Type of disk	d/d_0 min of arc	F/F_0
Single	10.6	3.5×10^{-3}
Double	12.0	8.0×10^{-4}
Double disks - 1 and 3	14.0	3.8×10^{-3}
Triple	14.0	2.6×10^{-4}
170 disk cone	14.0	3.1×10^{-4}

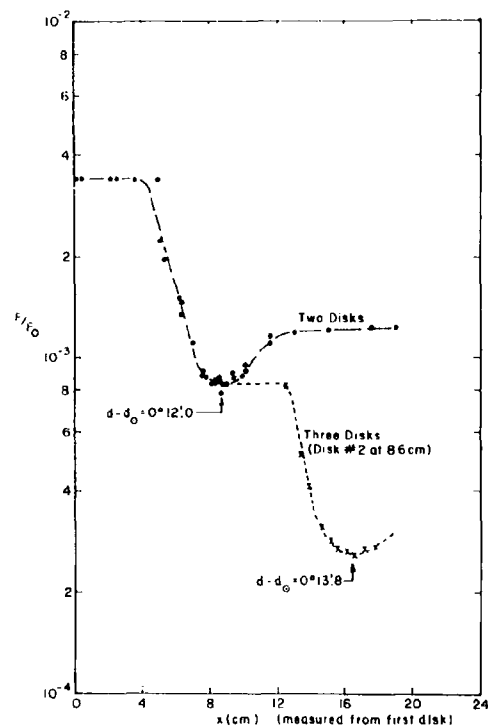


Fig. 9. Reduction of flux into an objective aperture by two- and three-disk occulting systems plotted as a function of the spacing between the disks. The experimental arrangement was the same as was used in the measurements shown in Fig. 6 with the first disk placed 76 cm from the objective aperture and the other disks placed x cm toward the aperture.

coronagraph and thus a reduction in the stray light in the coronagraph of approximately 2.6×10^{-4} . This represents an improvement of approximately a factor of 13 above the performance of the simple externally occulted disk coronagraph. Since this implies that the stray light in the complete coronagraph would be approximately 8×10^{-10} of the mean solar disk, such a design appears useful for a wide variety of both satellite and balloon-borne experiments.

We might say a word concerning the comparative advantages and disadvantages of the two occulting schemes—the multiple occulting disk and the toothed wheel. Purcell and Koomen have obtained a reduction in the shadow of a toothed-wheel occulter illuminated by a point source of approximately a factor of nine over the simple disk. This reduction compares favorably with that produced by the multiple disk. Our tests of a toothed wheel with an extended source subtending 32 min of arc produced an improvement of only a factor of two over the simple disk; however, we attribute the poor performance of our toothed wheel to irregularities

Table III. Comparison of Balloon-Borne and Satellite Coronagraphs

Item	Balloon	Satellite
Lifetime to meteoric exposure	-	10^6 to 10^7 sec in normal exposure 10^7 sec during meteor shower? Greater than 10^6 sec
Lifetime to x-ray and ultraviolet aging	-	-
Estimated observing period	8 hr (2.9×10^4 sec)	30 days (2.6×10^6 sec)
Data recording	Photographic, recovered	Telemetry of scanned image
Information content per image	50 intensity grades over 2.8×10^7 locations $(1.7 \times 10^6$ bits per photograph)	Same
Information rate	2.8×10^7 bits per sec assuming a 1-min exposure	20 bits per sec (total rate of information processing of OS-1)
Information content per flight	8.2×10^6 bits	2.6×10^6 bits
Number of images per flight	1.8×10^7	1.5×10^7
Time required to produce one image	60 sec	8.5×10^3 sec (2.4 hr)

in the structure of the teeth. This difference immediately points to a disadvantage of the toothed occulting disk—the difficulty in making a toothed wheel accurately enough to realize the full capabilities of the apodized occulting disk. The relative ease of fabricating accurately machined disks of controlled diameter for a multiple occulting disk is, however, compensated by a disadvantage of the multiple occulting scheme—the series of disks must all be accurately aligned on the optic axis of the system.

Comparison of Externally Occulted Coronagraphs Carried in Balloons or Satellites

Since it is possible to construct a coronagraph having an instrumental background only slightly different from that encountered during total solar eclipse, it is wise to compare the advantages and disadvantages of such an instrument when carried either on a satellite or on a balloon (Table III). Since both devices would be limited by the level of internally scattered light, both can be expected to detect the corona out to approximately six solar radii.

Perhaps the most remarkable difference between the two systems is the length of the observing periods. Another important difference exists in the rate at which they gather images of the corona. Assuming that both coronagraphs have an angular resolution of one minute of arc, we find that approximately 2×10^7 image points exist in the field. If we are to distinguish 50 intensity grades at each one of these locations, six bits per location (1.7×10^6 bits per complete image of the corona) are required. Although the present satellites suffer from their low data handling capacity (20 bits per second for OS-1), both systems gather approximately the same number of images per flight. Clearly, the second generation satellites, with their vastly improved telemetry systems, will be able to carry a coronagraph which can produce images of the corona at the same rate as the balloon-borne version. At the present time, however, the two coronagraphs can per-

form two complimentary and important functions. The balloon-borne instrument, being capable of producing fairly rapid photographs for a relatively short period, can give information on the transient phenomena; the satellite-borne instrument, on secular changes. Without both types of information our knowledge of the solar corona will be severely limited.

References

1. B. Lyot, C. R. Acad. Sci. Paris **191**, 831 (1930).
2. B. Lyot, C. R. Acad. Sci. Paris **193**, 1169 (1931).
3. B. Lyot, Monthly Notices Roy. Astron. Soc. **99**, 580 (1939).
4. I.G.Y., *Solar Activity Maps* (Pergamon Press, New York, 1961), Series D-2, Ann. of I.G.Y., Vol. 22.
5. G. Wierick and J. Axtell, *Astrophys. J.* **126**, 253 (1957).
6. G. Newkirk, Jr., G. W. Curtis, and K. Watson, I.G.Y., *Solar Activity Report Series No. 1* (1958).
7. A. Dollfus, C. R. Acad. Sci. Paris **247**, 12 (1958).
8. G. Newkirk, Jr., Paris Symposium on Radio Astronomy (ed. R. N. Bracewell, Stanford, 1959).
9. A. Dollfus, C. R. Acad. Sci. Paris **249**, 2722 (1959).
10. J. L. Leroy, Ann. d'Astrophys. **23**, 567 (1960).
11. E. E. Volz, Ber. Deut. Wetterdienstes **2**, No. 13 (1951).
12. G. Newkirk, Jr., *J. Opt. Soc. Am.* **46**, 1028 (1956).
13. G. Newkirk, Jr., and J. A. Eddy, *Nature* **194**, 638 (1962).
14. E. P. Ney, W. F. Hueb, P. J. Kellogg, W. Stein, and E. Gillett, *Astrophys. J.* **133**, 616 (1961).
15. M. Born, *Optik* (Springer, Berlin, 1933), § 81.
16. G. F. J. Garbick, *Handbuch der Physik*, ed. S. Flügge (Springer-Verlag, Berlin, 1958), Vol. 26, § 12.
17. N. J. Kreidl, *J. Opt. Soc. Am.* **35**, 219 (1945).
18. J. W. Evans, private communication.
19. T. E. Rodgers, paper presented at Spring Meeting, Optical Society of America, 3 April 1959.
20. J. W. Evans, *J. Opt. Soc. Am.* **38**, 1038 (1948).
21. G. Newkirk, Jr., and J. A. Eddy, *Sky and Telescope* **24**, 77 (1962).
22. B. Roizen-Dossier, *Astronomical Optics and Related Subjects*, ed. Z. Kopal (North Holland, Amsterdam, 1956), § 16.
23. R. Barakat, *J. Opt. Soc. Am.* **52**, 261 (1962).
24. M. Born and E. Wolf, *Principles of Optics* (Pergamon Press, New York, 1959), § 5.2.
25. J. D. Porech and M. J. Koonen, paper presented at Spring Meeting, Optical Society of America, 11-17 March 1962.
26. W. M. Alexander, C. W. McCracken, and H. E. LaGow, *J. Geophys. Research* **66**, 3970 (1961).